Markus Hautakorpi and Matti Kaivola. 2005. Modal analysis of M-type-dielectric-profile optical fibers in the weakly guiding approximation. Journal of the Optical Society of America A, volume 22, number 6, pages 1163-1169.

Modal analysis of M-type-dielectric-profile optical fibers in the weakly guiding approximation

Markus Hautakorpi and Matti Kaivola

Optics and Molecular Materials, Helsinki University of Technology, P.O.Box 3500, FI-02015 HUT, Finland

Received October 6, 2004; accepted November 29, 2004

We study the applicability of the weakly guiding approximation (WGA) to the modal analysis of an M-type optical fiber in which a ring-shaped core lies between two uniform cladding layers. Besides being dependent on the refractive indices, the accuracy of the approximation is shown to be substantially affected by the transverse dimensions of the core. The accuracy is characterized by calculating an overlap integral between the exact and WGA-approximated modal fields. Fibers that have an inner cladding similar to the outer cladding, or similar to vacuum, are considered in detail. The feasibility of the WGA in determining the fiber parameters for single-mode guidance is also discussed. © 2005 Optical Society of America

OCIS codes: 060.2310, 060.2340, 060.2430, 260.2110.

1. INTRODUCTION

The guided modes of M-type-dielectric-profile optical fibers have attracted attention during the past years in several applications. If the inner cladding is missing, i.e., the volume inside the core is empty, the fiber can be used to guide atoms along the hollow core.[1–3] In such a hollow optical fiber (HOF) (see Fig. 1) the atoms are confined in the dark near the fiber axis by repulsive dipole interaction between the atoms and the evanescent wave of the guided light, which is assumed to be detuned toward the blue from the atomic resonance. The output beam from the fiber can as well be used to guide and to trap atoms.[4,5] Fiber lasers based on M-type fibers[6,7] have been demonstrated, and just recently HOF has been used to excite resonances in a spherical microresonator.[8] In fiber-optical telecommunications HOF can serve as a modal filter[9] or as a mode converter.[10,11] There are also other M-type fibers of interest, such as the annular-core fiber (ACF),[12–14] in which both of the claddings have the same index of refraction (also known as the ring-core fiber). The self-imaging property of a suitable-length ACF[15] was recently applied to phase locking of a circular array of fiber lasers.[16,17]

For conventional optical fibers the weakly guiding approximation (WGA) states that if the refractive-index difference between the core and the cladding is small, i.e., if $\Delta n_{1,2}=n_1-n_2\ll 1$, the modal fields can be assumed to be linearly polarized in the transverse plane of the fiber.[18] The modes obtained under the WGA are hence denoted $LP_{m,p}$ modes, to be distinguished from the exact vectorial $EH_{l,p}$ and $HE_{l,p}$ hybrid modes (or the $TE_{0,p}$ and $TM_{0,p}$ modes). The accuracy of the WGA is dictated essentially by the value of $\Delta n_{1,2}$, and a dependence on the core dimension becomes an issue only through a modal cutoff. Due to its mathematical simplicity, the WGA is often applied also to M-type fibers having a small value of $\Delta n_{1,2}$. For an ACF such an approximation would seem to be justified by the fact that the refractive-index differences at both of the core–cladding boundaries are then small, but for an HOF with a large index difference at the inner boundary, such an approach is not necessarily appropriate. Nevertheless, HOFs have been widely studied by use of the WGA, and the description has proven to work well when compared with rigorous vectorial calculations[19] and with experimental observations of some guided modes.[1] From these individual cases of agreement one cannot, however, deduce the range of fiber parameters for which the WGA will in general yield acceptable results.

In the first part of this paper, we show that the transverse dimensions of the ring-shaped core will have a major influence on the accuracy of the WGA in addition to the effect of the refractive-index differences. A significant reduction in the accuracy can be seen in a fiber with a core thickness of a few wavelengths and an inner-cladding radius much larger than the wavelength. In such a case, for example, the fundamental hybrid mode $HE_{1,1}$ will no longer have purely linear polarization, which makes the description in terms of a strictly linearly polarized $LP_{0,1}$ mode unsatisfactory. To establish the range of fiber parameters within which the WGA can successfully be applied to ACFs and HOFs, we compare some low-order $LP_{m,p}$ modes with the corresponding superposition of the rigorous vector modes by calculating the overlap between the modal fields.

In the second part of the paper we discuss the feasibility of the WGA in finding the fiber parameters for single-mode propagation. The cutoff for the second lowest vector mode $TE_{0,1}$ is degenerate with that of the $LP_{1,1}$ mode in an M-type fiber,[20,21] and thus it suffices to consider the cutoffs of the fundamental modes $LP_{0,1}$ and $HE_{1,1}$.

The paper is organized as follows. In Section 2 we outline the derivation of the characteristic equations from Helmholtz's wave equation both rigorously and under the WGA. A simple measure is then presented to allow for

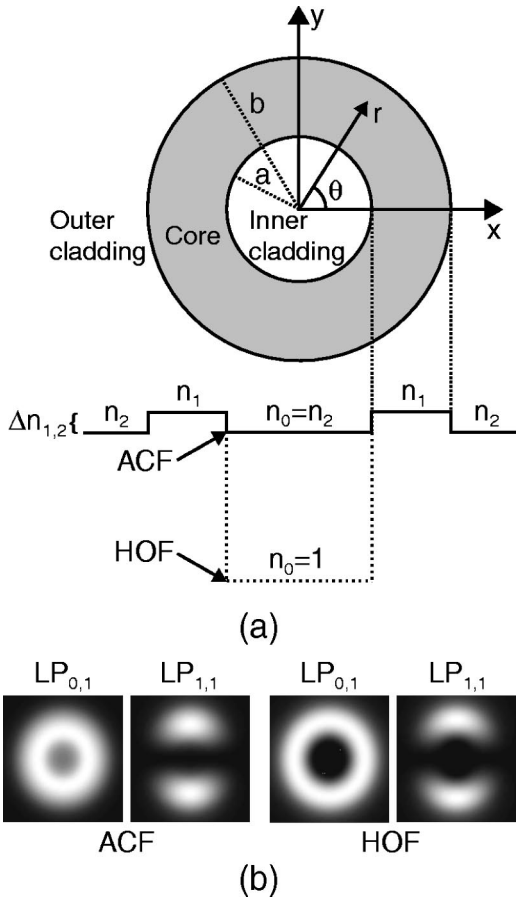

Fig. 1. (a) Schematic cross section of an M-type fiber, as defined here, with an inner and outer radius a and b of the core, respectively. Below are shown the refractive-index profiles of an annular-core fiber (ACF) and a hollow optical fiber (HOF) for which the inner claddings have the refractive index of that of the outer cladding (of infinite extent) and of vacuum, respectively. The step-index profile of a conventional optical fiber can be obtained on taking the limit $a \to 0$. (b) Transverse intensity profiles of the two lowest-order $\mathrm{LP}_{m,p}$ modes calculated for $a=2$ μm, $b=6$ μm, $n_1=1.46$, $n_2=1.45$, and wavelength $\lambda=1.55$ μm.

comparison of the electric field patterns given by these two formalisms. In Section 3 we apply the measure to investigate the accuracy of the WGA for some low-order modes in HOFs and ACFs. The exact and the WGA cutoff equations are considered in Section 4. Summary and discussion are presented in Section 5.

2. CHARACTERISTIC EQUATIONS AND CONSTRUCTION OF LINEARLY POLARIZED MODES

The exact time-harmonic vector modes of an M-type fiber are found as solutions to Helmholtz's wave equation, which in the geometry of Fig. 1 is most conveniently solved in cylindrical coordinates. The longitudinal component of the electric and magnetic field of a guided mode propagating in the positive z direction will then be of the general form $F(r,\theta,z;t)=F(r,\theta)\exp[i(\omega t-\beta z)]$, where β is the propagation constant, ω is the angular frequency of light, and t denotes time. The field amplitude F can be written as[22]

$$F(r,\theta)=\begin{cases} C_1 I_l(vr)\sin(l\theta+\phi), & r\leqslant a \\ [C_2 J_l(ur)+C_3 N_l(ur)]\sin(l\theta+\phi), & a<r<b \\ C_4 K_l(wr)\sin(l\theta+\phi), & b\leqslant r \end{cases}. \tag{1}$$

Here the functions J_l and N_l are Bessel functions of the first and second kind of the order l, respectively. Similarly, I_l and K_l denote modified Bessel functions of the first and second kind of the order l, respectively. The parameters v, w, and u are given by $v=(\beta^2-k^2n_0^2)^{1/2}$, $w=(\beta^2-k^2n_2^2)^{1/2}$, and $u=(k^2n_1^2-\beta^2)^{1/2}$, with k denoting the wave number in free space. The parameter ϕ is an arbitrary phase angle and $C_1,\ldots,C_4$ are constants.

The field in Eq. (1) is usually chosen to describe the longitudinal component E_z of the electric field.[1] The corresponding magnetic field H_z is obtained from this expression by replacing "sin" with "cos" and introducing another set of coefficients $C_5,\ldots,C_8$. The remaining transverse field components, denoted by the subscript t, can then be derived from the equations[23]

$$\mathbf{E}_t(r,\theta)=\frac{i}{\beta^2-k^2n_j^2}[\beta\nabla_t E_z(r,\theta)-\mu_j\omega\mathbf{u}_z\times\nabla_t H_z(r,\theta)],$$

$$\mathbf{H}_t(r,\theta)=\frac{i}{\beta^2-k^2n_j^2}[\beta\nabla_t H_z(r,\theta)+\epsilon_j\omega\mathbf{u}_z\times\nabla_t E_z(r,\theta)], \tag{2}$$

where $j=0$, 1, 2 denote the regions in the transverse dielectric profile of the fiber [see Fig. 1(a)], and where $\mu_j\approx\mu_{\mathrm{vac}}$ and $\epsilon_j=\epsilon_{\mathrm{vac}}n_j^2$ are, respectively, the permeability and permittivity of the region, with μ_{vac} and ϵ_{vac} being the corresponding values in vacuum. The explicit form of the differential operator is $\nabla_t=\mathbf{u}_r(\partial/\partial r)+\mathbf{u}_\theta(\partial/r\,\partial\theta)$, where $\mathbf{u}_r$ and $\mathbf{u}_\theta$, along with $\mathbf{u}_z$ in Eq. (2), stand for the unit vectors of the coordinate system. The transverse components turn out to have the separable forms

$$E_r(r,\theta)=E_r(r)\sin(l\theta+\phi),$$

$$E_\theta(r,\theta)=E_\theta(r)\cos(l\theta+\phi),$$

$$H_r(r,\theta)=H_r(r)\cos(l\theta+\phi),$$

$$H_\theta(r,\theta)=H_\theta(r)\sin(l\theta+\phi). \tag{3}$$

By demanding continuity of the tangential components E_z, E_θ, H_z, and H_θ over the core boundaries at $r=a$ and $r=b$, one can construct a matrix equation of the form $\mathbf{Ax}=0$, where the vector $\mathbf{x}$ contains the coefficients $C_1,C_2,\ldots,C_8$, and the matrix $\mathbf{A}$ reads

$$\mathbf{A}=\begin{bmatrix}
I_l(va) & -J_l(ua) & -N_l(ua) & 0 & 0 & 0 & 0 & 0\\
\frac{l\beta}{av^2}I_l(va) & \frac{l\beta}{au^2}J_l(ua) & \frac{l\beta}{au^2}N_l(ua) & 0 & \frac{-\omega\mu}{v}I_l'(va) & \frac{-\omega\mu}{u}J_l'(ua) & \frac{-\omega\mu}{u}N_l'(ua) & 0\\
0 & 0 & 0 & 0 & I_l(va) & -J_l(ua) & -N_l(ua) & 0\\
\frac{\omega\epsilon_0}{v}I_l'(va) & \frac{\omega\epsilon_0}{u}J_l'(ua) & \frac{\omega\epsilon_0}{u}N_l'(ua) & 0 & \frac{-l\beta}{av^2}I_l(va) & \frac{-l\beta}{au^2}J_l(ua) & \frac{-l\beta}{au^2}N_l(ua) & 0\\
0 & J_l(ub) & N_l(ua) & -K_l(wb) & 0 & 0 & 0 & 0\\
0 & \frac{-l\beta}{bu^2}J_l(ub) & \frac{-l\beta}{bu^2}N_l(ub) & \frac{-l\beta}{bw^2}K_l(wb) & 0 & \frac{\omega\mu}{u}J_l'(ub) & \frac{\omega\mu}{u}N_l'(ub) & \frac{\omega\mu}{w}K_l'(wb)\\
0 & 0 & 0 & 0 & 0 & J_l(ub) & N_l(ub) & -K_l(wb)\\
0 & \frac{-\omega\epsilon_1}{u}J_l'(ub) & \frac{-\omega\epsilon_1}{u}N_l'(ub) & \frac{-\omega\epsilon_2}{w}K_l'(wb) & 0 & \frac{l\beta}{bu^2}J_l(ub) & \frac{l\beta}{bu^2}N_l(ub) & \frac{l\beta}{bw^2}K_l(wb)
\end{bmatrix}. \quad (4)$$

Here the prime denotes differentiation with respect to the radial coordinate. The propagation constants β of the modes are given by the roots of the characteristic equation obtained by requiring that the determinant of this matrix vanish. The values of the coefficients $C_1,\ldots,C_8$ are then assigned by fixing the value of one of them, say C_8, and then applying Gaussian elimination to the original matrix equation $\mathbf{Ax}=0$. For the $TM_{0,p}$ modes, however, the coefficients $C_5,\ldots,C_8$ equal zero, and one proceeds by first fixing the value of C_4.

In the WGA the expression in Eq. (1) can be directly taken to represent a transverse electric field of a mode[22] $\tilde{E}\equiv F$ as in the analysis of conventional weakly guiding fibers,[18] with the tilde here referring to a quantity in the WGA. The WGA assumes that the refractive-index differences over the boundaries at $r=a$ and $r=b$ are so small that the transverse field components can be taken to pass continuously over these boundaries. Consequently, the first derivative of $\tilde{E}_t$ with respect to the radial coordinate will be continuous there as well. These boundary conditions can be collected by use of Eq. (1) as

$$\frac{\tilde{v}I_m'(\tilde{v}a)}{I_m(\tilde{v}a)}-\frac{\tilde{u}\tilde{C}_2J_m'(\tilde{u}a)+\tilde{u}\tilde{C}_3N_m'(\tilde{u}a)}{\tilde{C}_2J_m(\tilde{u}a)+\tilde{C}_3N_m(\tilde{u}a)}=0, \quad (5)$$

$$\frac{\tilde{w}K_m'(\tilde{w}b)}{K_m(\tilde{w}b)}-\frac{\tilde{u}\tilde{C}_2J_m'(\tilde{u}b)+\tilde{u}\tilde{C}_3N_m'(\tilde{u}b)}{\tilde{C}_2J_m(\tilde{u}b)+\tilde{C}_3N_m(\tilde{u}b)}=0. \quad (6)$$

On substituting $\tilde{C}_2$ from Eq. (5) into Eq. (6), the latter can be considered a characteristic equation for the $LP_{m,p}$ modes. A root of this equation yields the propagation constant $\tilde{\beta}$ of a mode, for which the coefficients $\tilde{C}_1,\ldots,\tilde{C}_4$ can then be found from Eqs. (1), (5), and (6).

Generally, an $LP_{m,p}$ mode corresponds to a superposition of the hybrid modes $EH_{m-1,p}$ and $HE_{m+1,p}$, which in a conventional optical fiber with a small value of $\Delta n_{1,2}$ have nearly degenerate propagation constants. The exceptions to this superposition rule are such that an $LP_{0,p}$ mode corresponds to the $HE_{1,p}$ mode and an $LP_{1,p}$ mode to the superposition of the odd (even) $HE_{2,p}$ mode and the $TE_{0,p}(TM_{0,p})$ mode.[1,23] In such a construction, which is here generalized to an M-type fiber, the vector modes are blended to yield a vanishing transverse component for the electric field,[24] say, in the x direction. The resulting field will then be polarized essentially in the y direction, and we set $\phi=0$ in Eq. (1) for both constitutive vector modes (for the $TM_{0,p}$ mode and the even $HE_{2,p}$ mode we choose $\phi=-\pi/2$). Neglecting the small longitudinal component will result in a field that is very close to the corresponding scalar-field $LP_{m,p}$ mode (taken to stand for the y component of the electric field), for which the expression is, however, considerably easier to obtain.

The above approach is, on the other hand, equivalent to the requirement that the transverse components E_r^- and E_θ^- of the $EH_{m-1,p}$ mode (or the nonvanishing component for the modes $TE_{0,p}$ and $TM_{0,p}$) and E_r^+ and E_θ^+ of the $HE_{m+1,p}$ mode have similar radial dependencies. This can be seen, assuming $m>1$, for example, by first resolving the Cartesian components of the superposed field by use of Eq. (3) as

$$\begin{aligned}\tilde{E}_x(r,\theta)\approx&-E_r^-(r)\sin[(m-1)\theta]\cos\theta-E_\theta^-(r)\\&\times\cos[(m-1)\theta]\sin\theta+E_r^+(r)\sin[(m+1)\theta]\\&\times\cos\theta-E_\theta^+(r)\cos[(m+1)\theta]\sin\theta,\end{aligned} \quad (7)$$

$$\begin{aligned}\tilde{E}_y(r,\theta)\approx&-E_r^-(r)\sin[(m-1)\theta]\sin\theta+E_\theta^-(r)\\&\times\cos[(m-1)\theta]\cos\theta+E_r^+(r)\sin[(m+1)\theta]\\&\times\sin\theta+E_\theta^+(r)\cos[(m+1)\theta]\cos\theta,\end{aligned} \quad (8)$$

where an explicit minus sign is added in front of E_r^- in both equations to account for a phase difference π between E_r^- and E_θ^-. Then, by assuming a common form $\hat{E}$ for the radial parts $E_r^\pm$ and $E_\theta^\pm$, the terms in Eq. (7) will add up destructively, yielding $\tilde{E}_x=0$. In contrast the constructive addition of the y components in Eq. (8) produces the expression

$$\tilde{E}_y(r,\theta) = 2\hat{E}(r)\sin(m\theta + \pi/2), \quad (9)$$

which is similar to Eq. (1) (with the phase angle $\tilde{\phi} = \pi/2$) that was used above to describe the transverse field of an $LP_{m,p}$ mode. In this construction both of the constituent vector modes carry the same amount of power, hence the factor 2 on the right-hand side of Eq. (9).

The foregoing notion that an $LP_{m,p}$ mode corresponds to a sum of equal-power vector modes can be taken as the basis for a procedure of evaluating the accuracy of the WGA. By normalizing the power in both of the vector modes according to the relation $\int\int|\mathbf{E}|^2 r\mathrm{d}r\mathrm{d}\theta = 1/2$, with the electric field vector $\mathbf{E} = E_r\mathbf{u}_r + E_\theta\mathbf{u}_\theta + E_z\mathbf{u}_z$ given by Eqs. (1)–(3), the superposition field will carry unit power (the $HE_{1,1}$ mode can be normalized directly to unity). Similarly the normalization of the corresponding $LP_{m,p}$ mode can be done by use of the relation $\int\int|\tilde{\mathbf{E}}|^2 r\mathrm{d}r\mathrm{d}\theta = 1$, where the electric field is expressed as $\tilde{\mathbf{E}} = F\mathbf{u}_y$ through Eq. (1), with $\mathbf{u}_y$ denoting a unit vector in the y direction. A mismatch between an exact modal field and the corresponding scalar-field approximation can then be revealed by taking an inner product between them and subsequently integrating the result over a transverse plane of the fiber. By denoting the electric fields of the vector modes by $\mathbf{E}^-$ and $\mathbf{E}^+$, one can formulate this procedure as

$$W = \int_0^\infty \int_0^{2\pi} [\mathbf{E}^-(r,\theta) + \mathbf{E}^+(r,\theta)]^* \cdot \tilde{\mathbf{E}}(r,\theta) r\mathrm{d}r\mathrm{d}\theta, \quad (10)$$

which defines a quantity W to characterize the accuracy of the WGA. An upper limit to the squared modulus $|W|^2$ is unity as a result of the chosen normalization of the fields. In such a case an $LP_{m,p}$ mode would exactly describe a modal field in the fiber, both in polarization and amplitude. Any deviation from this situation, either in polarization or amplitude (and implicitly also in the propagation constants), will be reflected in the value of $|W|^2$ by its reduction below unity.

3. MODAL DESCRIPTION OF LIGHT FIELDS IN ANNULAR-CORE AND HOLLOW OPTICAL FIBERS

In this section we apply the above formalism to study modal fields in ACFs and HOFs with their transverse dimensions selected according to applications in telecommunications and in atom guiding, respectively. For ACFs we select the wavelength of light to be the telecommunication wavelength $\lambda = 1.55\ \mu$m, whereas for HOFs we choose $\lambda = 780$ nm, which would correspond to the guiding of Rb atoms. To begin with we give in Fig. 2 an illustration of the effect of the core dimension of an HOF on the accuracy of describing the fundamental $HE_{1,1}$ mode as an $LP_{0,1}$ mode. In Fig. 2(a) the inner-cladding radius a is first taken to be zero, which corresponds to the case of a conventional step-index optical fiber. The $HE_{1,1}$ mode then has perfectly linear polarization, and the corresponding plot for the $LP_{0,1}$ mode coincides with the one presented, i.e., the accuracy parameter has the value of $|W|^2 = 1.00$. If a hole of radius $a = 8\ \mu$m is then introduced in the center of the structure as in Fig. 2(b), an HOF with a core thickness of a few wavelengths is formed. The polarization of the fundamental $HE_{1,1}$ mode is seen clearly to deviate from linear in such an HOF, and the amplitude distribution is far from being rotationally symmetric, both of which are features of the corresponding $LP_{0,1}$ mode shown in Fig. 2(c) for comparison. The number describing the accuracy of the WGA is now $|W|^2 = 0.84$.

Figure 3(a) shows the behavior of the quantity $|W|^2$ for some ACFs of different outer radii b of the core. Figure 3(b) shows the corresponding curves for HOFs. Four curves are plotted for each b as a function of the inner-cladding radius a by varying the refractive-index difference $\Delta n_{1,2}$ between the core and the outer cladding. In Fig. 3(a) the parameter $\Delta n_{1,2}$ ranges from 0.50% to 2.00%. For the smallest value $b = 10\ \mu$m, the $LP_{0,1}$ mode is very close to the $HE_{1,1}$ mode, causing the value of $|W|^2$ to be near unity for all the considered values of $\Delta n_{1,2}$. However, when the value of b is increased, a dip emerges in the curves for values of a a few wavelengths smaller than b. The depth of the dip scales with the values of $\Delta n_{1,2}$ and b, and near the bottom of the dip the $HE_{1,1}$ and $LP_{0,1}$ modes differ qualitatively as in Figs. 2(b) and 2(c). When a is very close to b, the accuracy is again recovered. In general, for a small $\Delta n_{1,2}$ (much smaller than would be allowed in a conventional fiber), the fundamental mode is essentially an $LP_{0,1}$ mode irrespective of the core dimensions, but for values on the order of $\Delta n_{1,2} \approx 2\%$ or higher, the core has to be much thicker (or thinner) than the-

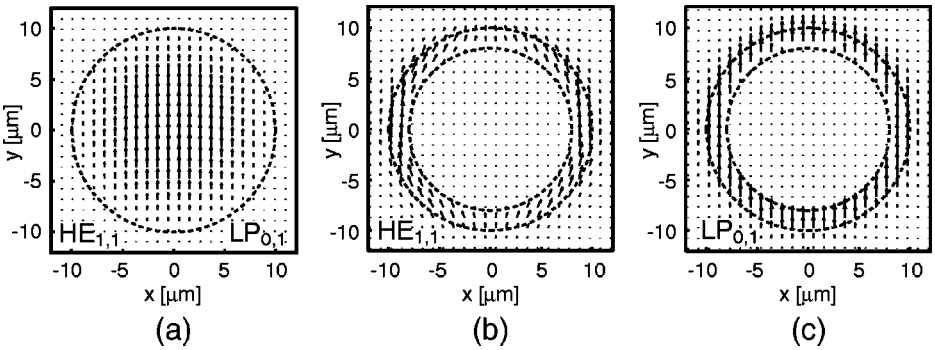

Fig. 2. Effect of the inner radius of the core on the polarization and amplitude of the fundamental mode. The fiber parameters are $\Delta n_{1,2} = 1.00\%$ and $b = 10\ \mu$m and the wavelength is $\lambda = 780$ nm. The core boundaries are shown by dashed circles. (a) $HE_{1,1}$ or $LP_{0,1}$ mode in a conventional step-index fiber. (b) $HE_{1,1}$ mode in an HOF with an inner radius of $a = 8\ \mu$m. (c) $LP_{0,1}$ mode of the fiber in Fig. 2(b) calculated by use of the WGA.

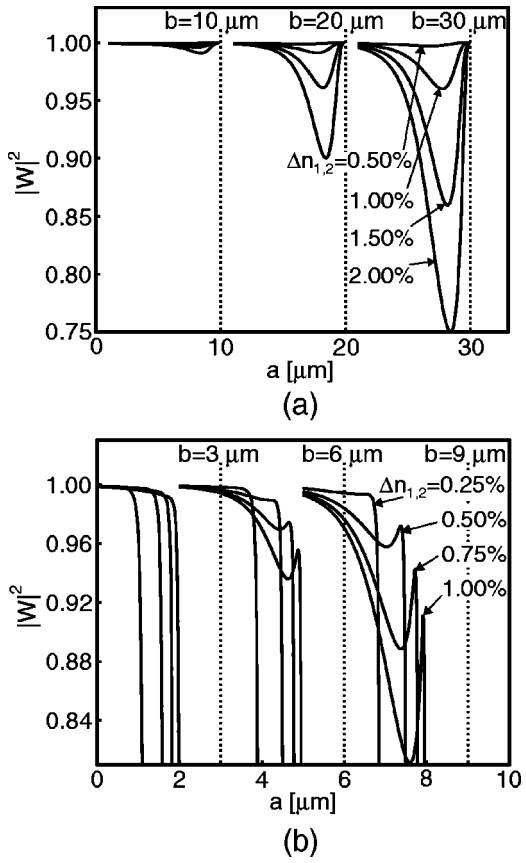

Fig. 3. Accuracy $|W|^2$ of the WGA in describing the $HE_{1,1}$ mode (a) in an ACF at $\lambda = 1.55$ μm and (b) in an HOF at $\lambda = 780$ nm with $n_2 = 1.45$ as a function of the inner radius a of the core. Three different outer radii b of the core, denoted by vertical dotted lines, are considered in both plots. The curves correspond to refractive-index differences increasing from top to down, as indicated.

wavelength, or altogether relatively small, for this to be true.

In HOFs intended for use as atom guides, the refractive-index difference and the core dimensions are typically smaller than in the ACF examples considered above, because the light field needs to be very smooth and intense on the fiber's inner surface. In Fig. 3(b) the highest value of b is thus chosen to be 9 μm with the parameter $\Delta n_{1,2}$ ranging from 0.25% to 1.00%. Qualitatively, the curves begin to behave similarly to those for the ACFs for small values of a. As a approaches b, the $HE_{1,1}$ mode reaches its cutoff before the $LP_{0,1}$ mode (see Section 4), causing the value of $|W|^2$ to drop sharply near the cutoff. Before this, the curve exhibits a dip similar to those with the ACFs of Fig. 3(a). Again the dip is more clearly visible in the larger fibers. As a rule one might say that for the values of $\Delta n_{1,2}$ considered here, the thickness of the core should not be less than $\approx b/2$ for the fundamental mode to be well described by an $LP_{0,1}$ mode, unless $\Delta n_{1,2}$ is very small, in which case being far from the cutoff is sufficient.

Figure 4 shows the corresponding plots for the second-order modal fields in the fibers of Fig. 3. The curves corresponding to the superposition of the odd $HE_{2,1}$ mode and $TE_{0,1}$ mode are solid, and those for the superposition of the even $HE_{2,1}$ mode and the $TM_{0,1}$ mode are dashed. In Fig. 4 the values of $|W|^2$ are in general much closer to unity than in Fig. 3, although the qualitative behavior is very similar. However, all the curves in Fig. 4(a) eventually bend down for very thin fiber cores because of the cutoffs for the $TE_{0,1}$ and $LP_{1,1}$ modes, which are degenerate.[20,21] In Fig. 4(b) the declines due to these cutoffs are more visible and one can see that the dashed curves fall off monotonically, whereas the solid curves rise slightly for some of the largest fibers, as in Fig. 3(b). In brief a second-order modal field can effectively be described as an $LP_{1,1}$ mode below modal cutoffs, if similar guidelines are applied in choosing the fiber parameters as with the fundamental modes above. Note that the analysis for an HOF with the other wavelength $\lambda = 1.55$ μm can be obtained by scaling a and b with the ratio of the wavelengths (≈ 2) in Figs. 3(b) and 4(b).

4. SINGLE-MODE M-TYPE FIBERS

In this section we consider the cutoffs of the modes considered in the previous section to determine how well the WGA works in finding the parameters for single-mode guidance in M-type fibers. The exact cutoff equation follows by requiring that the determinant of the matrix **A** in Eq. (4) vanish in the limit of $w \to 0$. The relevant cutoffs are then found from the equation

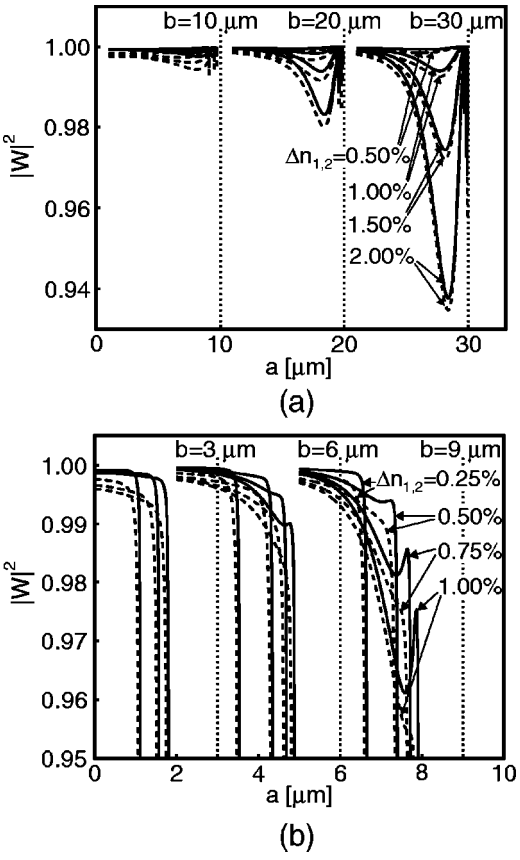

Fig. 4. Correspondence between $LP_{1,1}$ mode with the superposition of odd $HE_{2,1}$ and $TE_{0,1}$ (solid curves) and even $HE_{2,1}$ and $TM_{0,1}$ (dashed curves) modes in terms of the quantity $|W|^2$ as a function of the inner radius a of the core. The different outer radii b of the core, the wavelengths, and the refractive indices are as in Fig. 3. Second-order modes do not exist for $b = 3$ μm with $\Delta n_{1,2} = 0.25\%$; thus only three pairs of curves are given.

$$\left\{\left[\frac{1}{u}N_l'(ua)+\frac{1}{v}\frac{I_l'(va)}{I_l(va)}N_l(ua)\right]J_l(ub)-\left[\frac{1}{u}J_l'(ua)+\frac{1}{v}\frac{I_l'(va)}{I_l(va)}J_l(ua)\right]N_l(ub)\right\}\times\left\{\left[\frac{n_1^2}{u}N_l'(ua)+\frac{n_0^2}{v}\frac{I_l'(va)}{I_l(va)}N_l(ua)\right]J_l(ub)-\left[\frac{n_1^2}{u}J_l'(ua)+\frac{n_0^2}{v}\frac{I_l'(va)}{I_l(va)}J_l(ua)\right]N_l(ub)\right\}-\left(\frac{n_2 l}{a}\right)^2\left(\frac{1}{u^2}+\frac{1}{v^2}\right)^2\times[J_l(ua)N_l(ub)-J_l(ub)N_l(ua)]^2=0. \quad (11)$$

This equation is similar to the equation displayed in Ref. 1 with the difference that here none of the expressions in the square brackets explicitly depends on b. The cutoffs for the $TE_{0,p}$ ($TM_{0,p}$) modes are obtained by setting the first (second) term in the curly brackets equal to zero with $l=0$. For the cutoffs of the $HE_{1,p}$ (and the $EH_{1,p}$) modes one sets $l=1$ throughout the equation.

In the WGA the cutoff equation follows from Eq. (6) on taking the limit $\tilde{w}\to 0$. On substituting the coefficient $\tilde{C}_2$ from Eq. (5) and using the recurrence relations of the regular and modified Bessel functions,[25] one can cast the resulting equation in the form

$$\left[-\frac{1}{\tilde{u}}N_m(\tilde{u}a)+\frac{1}{\tilde{v}}\frac{I_m(\tilde{v}a)}{I_{m-1}(\tilde{v}a)}N_{m-1}(\tilde{u}a)\right]J_{m-1}(\tilde{u}b)-\left[-\frac{1}{\tilde{u}}J_m(\tilde{u}a)+\frac{1}{\tilde{v}}\frac{I_m(\tilde{v}a)}{I_{m-1}(\tilde{v}a)}J_{m-1}(\tilde{u}a)\right]N_{m-1}(\tilde{u}b)=0. \quad (12)$$

In this equation, one sets $m=0$ and $m=1$ for the $LP_{0,p}$ and $LP_{1,p}$ modes, respectively.

By comparing Eq. (12) with $m=1$ to the first two rows of Eq. (11) with $l=0$, one can see that the expressions become identical. In particular the cutoffs of the second lowest modes $LP_{1,1}$ and $TE_{0,1}$ are degenerate in any M-type fiber. For the fundamental modes with $m=0$ and $l=1$, however, Eqs. (12) and (11) will yield differing results. Figure 5 shows an example of the ratio of the cutoff wavelengths $\tilde{\lambda}_c$ and λ_c of the $LP_{0,1}$ and $HE_{1,1}$ modes, respectively, obtained from the two equations as a function of the refractive index n_0. A few values of the ratio a/b between the inner and outer radii of the core are considered. As the value of n_0 decreases from the value of n_1, the $HE_{1,1}$ mode will attain a finite cutoff wavelength slightly earlier than the $LP_{0,1}$ mode, yielding a high value for the ratio $\tilde{\lambda}_c/\lambda_c$. These cutoffs take place for the values[21]

$$n_{0,c}\approx[n_1^2-(b/a)^2(n_1^2-n_2^2)]^{1/2}, \quad (13)$$

which are marked in Fig. 5 as vertical dotted lines. Below this critical value the ratio of the cutoff wavelengths reaches a local minimum that is closer to unity in value and occurs nearer to $n_{0,c}$ for fibers with a high value of the ratio a/b. On the whole the WGA is seen to determine the cutoff wavelength more accurately for such fibers than for fibers with a small value of a/b.

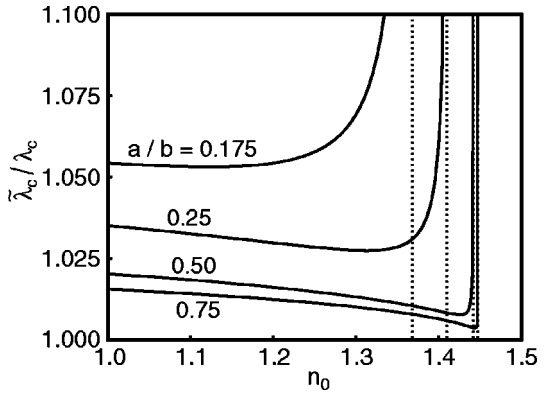

Fig. 5. Ratio of cutoff wavelengths $\tilde{\lambda}_c$ (WGA) and λ_c (exact) of the fundamental mode as a function of the refractive index n_0 of the inner cladding for different ratios between the inner and outer radii, a and b, respectively, of the core. The fixed refractive indices are $n_1=1.4525$ and $n_2=1.45$.

5. SUMMARY AND DISCUSSION

We have studied the effect of the transverse dimensions of an M-type fiber on the accuracy of modal analysis by use of the weakly guiding approximation (WGA). When the inner and outer claddings of the fiber have the same index of refraction, the $LP_{0,1}$ and $LP_{1,1}$ modes were shown to describe the modal field well for core thicknesses much above (or much below) the optical wavelength. On the other hand, a refractive index of unity of the inner cladding requires the core to be thicker than roughly half the outer radius of the core for the modal description obtained by means of the WGA to be accurate. For a fixed wavelength in general, the discrepancies are more significant in larger fibers, and the approximation is more accurate for the second-order modal fields than for the fundamental field. In addition, it was found that in the WGA, the cutoff wavelength for the fundamental mode can be most accurately determined if the ratio between the inner and outer radii of the fiber core is high, i.e., if the core is thin.

When applying a hollow single-mode fiber to guiding of cold atoms, the efficient transfer of the atoms into the fiber will strongly depend on the intensity distribution just outside the fiber. We note that in cases where the $LP_{0,1}$ mode well describes the rigorous $HE_{1,1}$ mode, the scalar diffraction calculation will bring out the true output field.[4,26] On the other hand when an incident light beam is coupled into an M-type fiber, the LP-mode approximation will predict inaccurate modal coupling efficiencies when $|W|^2$ differs from unity. This can be important, for instance, in calculations of the optimum pump-power coupling in an M-type-fiber laser,[6,7] since a thin-core fiber is required for single-radial mode propagation. A similar size requirement is found also in self-imaging applications of ACFs.[15,17] As regards optical fibers in general, the justification of the WGA often relies on the smallness of the refractive-index differences. Rigorous investigations, such as the work reported here, will then be valuable for justifying the approach selected for the modal analysis.

ACKNOWLEDGMENTS

This research was supported by the Academy of Finland. M. Hautakorpi acknowledges also the Jenny and Antti Wihuri fund and the Alfred Kordelin foundation for grants in the course of this work.

The corresponding author's e-mail address is Markus.Hautakorpi@hut.fi.

REFERENCES

1. H. Ito, K. Sakaki, T. Nakata, W. Jhe, and M. Ohtsu, "Optical potential for atom guidance in a cylindrical-core hollow fiber," Opt. Commun. **115**, 57–64 (1995).
2. H.-R. Noh and W. Jhe, "Atom optics with hollow optical systems," Phys. Rep. **372**, 269–317 (2002).
3. R. G. Dall, M. D. Hoogerland, D. Tierney, K. G. H. Baldwin, and S. J. Buckman, "Single-mode hollow optical fibres for atom guiding," Appl. Phys. B: Lasers Opt. **74**, 11–18 (2002).
4. S. H. Yoo, C. Won, J.-A. Kim, K. Kim, U. Shim, K. Oh, U.-C. Paek, and W. Jhe, "Diffracted near field of hollow optical fibre for a novel atomic funnel," J. Opt. B: Quantum Semiclassical Opt. **1**, 364–370 (1999).
5. Y.-I. Shin, M. Heo, J.-W. Kim, W. Shim, H.-R. Noh, and W. Jhe, "Diffraction-limited optical dipole trap with a hollow optical fiber," J. Opt. Soc. Am. B **20**, 937–941 (2003).
6. P. Glas, M. Naumann, A. Schirrmacher, and Th. Pertsch, "A neodymium doped hollow optical fiber laser for applications in sensing and laser guided atoms," Opt. Commun. **166**, 71–78 (1999).
7. P. Glas, M. Naumann, A. Schirrmacher, S. Unger, and Th. Pertsch, "Short-length 10-W cw neodymium-doped *M*-profile fiber laser," Appl. Opt. **37**, 8434–8437 (1998).
8. A. Nürenberg and G. Schweiger, "Excitation and recording of morphology-dependent resonances in spherical microresonators by hollow light guiding fibers," Appl. Phys. Lett. **84**, 2043–2045 (2004).
9. S. Choi, T. J. Eom, J. W. Yu, B. H. Lee, and K. Oh, "Novel all-fiber bandpass filter based on hollow optical fiber," IEEE Photonics Technol. Lett. **14**, 1701–1703 (2002).
10. S. Choi, K. Oh, W. Shin, C. S. Park, U. C. Paek, K. J. Park, Y. C. Chung, G. Y. Kim, and Y. G. Lee, "Novel mode converter based on hollow optical fiber for gigabit LAN communication," IEEE Photonics Technol. Lett. **14**, 248–250 (2002).
11. S. Choi and K. Oh, "A new LP_{02} mode dispersion compensation scheme based on mode converter using hollow optical fiber," Opt. Commun. **221**, 307–312 (2003).
12. B. C. Sarkar, P. K. Choudhury, and T. Yoshino, "On the analysis of a weakly guiding doubly clad dielectric optical fiber with an annular core," Microwave Opt. Technol. Lett. **31**, 435–439 (2001).
13. J. Marcou and S. Février, "Comments on 'On the analysis of a weakly guiding doubly clad dielectric optical fiber with an annular core'," Microwave Opt. Technol. Lett. **38**, 249–254 (2003).
14. P. K. Choudhury and R. A. Lessard, "An estimation of power transmission through a doubly clad optical fiber with an annular core," Microwave Opt. Technol. Lett. **29**, 402–405 (2001).
15. C. Y. H. Tsao, D. N. Payne, and W. A. Gambling, "Modal characteristics of three-layered optical fiber waveguides: a modified approach," J. Opt. Soc. Am. A **6**, 555–563 (1989).
16. M. Wrage, P. Glas, D. Fischer, M. Leitner, N. N. Elkin, D. V. Vysotsky, A. P. Napartovich, and V. N. Troshchieva, "Phase-locking of a multicore fiber laser by wave propagation through an annular waveguide," Opt. Commun. **205**, 367–375 (2002).
17. A. P. Napartovich and D. V. Vysotsky, "Phase-locking of multicore fibre laser due to Talbot self-reproduction," J. Mod. Opt. **50**, 2715–2725 (2003).
18. D. Gloge, "Weakly guiding fibers," Appl. Opt. **10**, 2252–2258 (1971).
19. P. R. Chaudhuri, C. Lu, and W. Xiaoyan, "Scalar model and exact vectorial description for the design analysis of hollow optical fiber components," Opt. Commun. **228**, 285–293 (2003).
20. I. V. Neves and A. S. C. Fernandes, "Modal characteristics for A-type and V-type dielectric profile fibers," Microwave Opt. Technol. Lett. **16**, 164–169 (1997).
21. I. V. Neves and A. S. C. Fernandes, "Modal characteristics for *W*-type and *M*-type dielectric profile fibers," Microwave Opt. Technol. Lett. **22**, 398–405 (1999).
22. H. Ito, K. Sakaki, T. Nakata, W. Jhe, and M. Ohtsu, "Optical guidance of neutral atoms using evanescent waves in a cylindrical-core hollow fiber: theoretical approach," Ultramicroscopy **61**, 91–97 (1995).
23. A. W. Snyder and J. D. Love, *Optical Waveguide Theory*, 1st ed. (Chapman & Hall, London, 1983).
24. D. Marcuse, *Theory of Dielectric Optical Waveguides*, 1st ed. (Academic, New York, 1974).
25. G. B. Arfken and H. J. Weber, *Mathematical Methods for Physicists*, 4th ed. (Academic, San Diego, Calif., 1995).
26. Y. Ni, N. Liu, and J. Yin, "Diffracted field distributions from the HE_{11} mode in a hollow optical fibre for an atomic funnel," J. Opt. B: Quantum Semiclassical Opt. **5**, 300–308 (2003).